Advanced Composite Materials
Publication details, including instructions for authors and subscription information:
http://www.tandfonline.com/loi/tacm20

The Thermal Stability and Elevated Temperature Mechanical Properties of Spray-Deposited SiCp/Al-11.7Fe-1.3V-1.7Si Composite

L. Hao [a], Y. Q. He [b], Na Wang [c], Z. H. Chen [d], Z. G. Chen [e], H. G. Yan [f] & Z. K. Xu [g]

[a] College of Materials Science and Engineering, Hunan University, Changsha 410082, People's Republic of China

[b] College of Mechanical Engineering, Huaihai Institute of Technology, Lianyungang 222005, People's Republic of China;, Email: haoliang2005abcd@126.com

[c] Department of Human Resources, Huaihai Institute of Technology, Lianyungang 222005, People's Republic of China

[d] College of Materials Science and Engineering, Hunan University, Changsha 410082, People's Republic of China

[e] College of Materials Science and Engineering, Hunan University, Changsha 410082, People's Republic of China

[f] College of Materials Science and Engineering, Hunan University, Changsha 410082, People's Republic of China

[g] College of Materials Science and Engineering, Hunan University, Changsha 410082, People's Republic of China, Department of Mechanical Engineering, Zhangjiajie Institute of Aviation Industry Vocational, Zhangjiajie, Hunan 427000, People's Republic of China

Version of record first published: 02 Apr 2012.

VSP

Advanced Composite Materials 18 (2009) 351–364

ADVANCED COMPOSITE MATERIALS
www.brill.nl/acm

The Thermal Stability and Elevated Temperature Mechanical Properties of Spray-Deposited SiC_p/Al–11.7Fe–1.3V–1.7Si Composite

L. Hao [a], Y. Q. He [b,*], Na Wang [c], Z. H. Chen [a], Z. G. Chen [a], H. G. Yan [a] and Z. K. Xu [a,d]

[a] College of Materials Science and Engineering, Hunan University, Changsha 410082, People's Republic of China

[b] College of Mechanical Engineering, Huaihai Institute of Technology, Lianyungang 222005, People's Republic of China

[c] Department of Human Resources, Huaihai Institute of Technology, Lianyungang 222005, People's Republic of China

[d] Department of Mechanical Engineering, Zhangjiajie Institute of Aviation Industry Vocational, Zhangjiajie, Hunan 427000, People's Republic of China

Received 2 October 2007; accepted 7 November 2008

Abstract

The thermal stability and elevated temperature mechanical properties of SiC_p/Al–11.7Fe–1.3V–1.7Si (Al–11.7Fe–1.3V–1.7Si reinforced with SiC particulates) composites sheets prepared by spray deposition (SD) → hot pressing → rolling process were investigated. The experimental results showed that the composite possessed high σ_b (elevated temperature tensile strength), for instance, σ_b was 315.8 MPa, which was tested at 315°C, meanwhile the figure was 232.6 MPa tested at 400°C, and the elongations were 2.5% and 1.4%, respectively. Furthermore, the composite sheets exhibited excellent thermal stability: the hardness showed no significant decline after annealing at 550°C for 200 h or at 600°C for 10 h. The good elevated temperature mechanical properties and excellent thermal stability should mainly be attributed to the formation of spherical α-$Al_{12}(Fe, V)_3Si$ dispersed phase particulates in the aluminum matrix. Furthermore, the addition of SiC particles into the alloy is another important factor, which the following properties are responsible for. The resultant Si of the reaction between Al matrix and SiC particles diffused into Al matrix can stabilize α-$Al_{12}(Fe, V)_3Si$ dispersed phase; in addition, the interface (Si layer) improved the wettability of Al/SiC_P, hence, elevated the bonding between them. Furthermore, the fine Al_4C_3 phase also strengthened the matrix as a dispersion-strengthened phase. Meanwhile, load is transferred from Al matrix to SiC particles, which increased the cooling rate of the melt droplets and improved the solution strengthening and dispersion strengthening.

Keywords

Spray deposition, elevated temperature properties, thermal stability, SiC particle

* To whom correspondence should be addressed. E-mail: haoliang2005abcd@126.com
Edited by JSCM and KSCM

DOI:10.1163/156855109X434766

1. Introduction

In 1986, Skinner used plate fluid cast technology (PFC) to develop an Al–Fe–V–Si system heat resistant aluminum alloy [1], which has been used for temperatures up to 400°C, so it is believed to be one of the best candidates for titanium alloys. Rapid solidification (RS) Al–Fe–V–Si system heat resistant aluminum alloy exhibits low density, excellent ambient and elevated-temperature properties, outstanding heat stability, ductibility and fracture toughness, so considerable research effort have been made [2–9].

The study of the mechanical properties and the thermal stability of Al–8.4Fe–1.3V–1.7Si indicated that the high temperature mechanical properties of Al–Fe–V–Si alloy exposed at 753 K for 500 h had no evident change compared with ambient temperature mechanical properties of the alloy, but they dropped remarkably after heat exposure above 753 K. The α-$Al_{12}(Fe, V)_3Si$ metastable phase did not undergo evident coarsening after heat exposure at 753 K for 500 h. Recrystallization in α-Al matrix occurred, the aggregation of α-$Al_{12}(Fe, V)_3Si$ occurred at the grain boundaries at 873 K [10].

The preparation methods for SiC_P/Al–Fe–V–Si composite include rapidly solidification/powder metallurgy (RS/PM) and spray deposition (SD). In previous works, researches emphasized on RS/PM of the composite, the process of which are relatively complex, while the multi-layer spray deposition was involved in rarely and the sheet of the composite had been investigated hardly. In this paper, sheets of the SiC_P/Al–11.7Fe–1.3V–1.7Si composite were prepared by the method of advanced multi-layer spray deposition. The microstructures, the mechanical properties at elevated temperature and thermal stability of the composite were investigated.

The aim of this article is to describe the elevated temperature mechanical properties and the thermal stability of SiC_P/Al–11.7Fe–1.3V–1.7Si composite and set forth the correlations between the microstructure and excellent mechanical properties of the composite, furthermore, provide the reinforcement mechanism of SiC particles.

2. Methods

The nominal composition of Al–Fe–V–Si alloy in this study is Al–11.7Fe–1.3V–1.7Si (mass percent). The reinforcement phase β-SiC particles with hexagonal lattice introduced into the alloy was produced by Weifang Aochuan Micro Podwer Co. Ltd. in China. It took up a volume fraction of 15% and mean size of about 10 μm. The composite preforms were firstly fabricated by a self-developed spray deposition equipment. The processing parameters of the spray deposition experiments are shown in Table 1. The density of the as-deposited preforms was 88% measured by Archimedes' method.

Hot pressing was used for densification of the composite performs. The as-deposited performs were cylinders with the size of 300 mm in diameter and 400 mm in height. The preforms were turned to 155 mm in diameter before hot working. The

Table 1.
Process parameters of the multi-layer spray deposition [21]

Atomization temperature (K)	1223–1373
Diameter of the melt stream (mm)	3.2–3.6
Spray height (mm)	200–350
Rotation speed of the substrate (rev min^{-1})	100–350
Scanning velocity of the nozzle (s)	10–30
Pressure of atomization gas (MPa)	0.7–0.9

as-turned billets were heated up to 450°C and then hot pressed to a column with the diameter of 165 mm. The temperature of the hot pressing model was heated up to 410°C. The as-pressed columns were turned to 155 mm in diameter and then hot-pressed again.

The optimum temperature for hot rolling was 490°C, which was different from the unreinforced alloys. Before hot rolling, the billet was preheated for 1 h. The pass reduction was about 10%. The billet was heated for 10 min/pass. The obtained SiC_P/Al–11.7Fe–1.3V–1.7Si composite sheets were 0.6–0.8 mm in thickness.

The annealing test was performed on the HBRVU-187.5 hardness tester produced by Shanghai Material Testing Machine Factory. Brinell hardness (HB) was measured under the condition of 613 N for 30 s. The specimens were cut from the rolled SiC_P/Al–11.7Fe–1.3V–1.7Si composite. The annealing temperatures were 350°C, 450°C, 550°C, 600°C and 620°C, respectively. The annealing times were 1, 3, 5, 10, 20, 30, 50, 70, 100, 150 and 200 h for 350°C, 450°C and 550°C, respectively. When annealing at 600°C, one sample was taken out every hour from 1 h to 10 h; when annealing at 620°C, the products were sampled every hour from 1 h to 5 h.

Tensile specimens with the tensile axis parallel to the longitudinal direction were machined from sheets of the as-rolled composite. The mechanical properties of the composite were examined by means of tensile testing with a tensile velocity of 0.5 mm/min. The high temperature tensile tests were performed on WDW-E200 computer-controlled universal material testing machine which was produced by Shijin Group Inc. in China. GB/T 228-2002 of China was adopted as the testing standard of the tensile tests. The microstructures of the composite were examined by Siemens D-5000 X-ray diffraction (XRD), H-800 transmission electron microscopy (TEM) manufactured by Hitachi and JEM-3010 high resolution transmission electron microscopy (HREM) which was manufactured by JEOL.

3. Results and Discussion

3.1. The Microstructures of the Composite

It can be seen in Fig. 1 that the XRD patterns of the composite as-deposited, as-pressed and as-rolled are similar, the main peaks correspond to β-SiC phase, α-Al

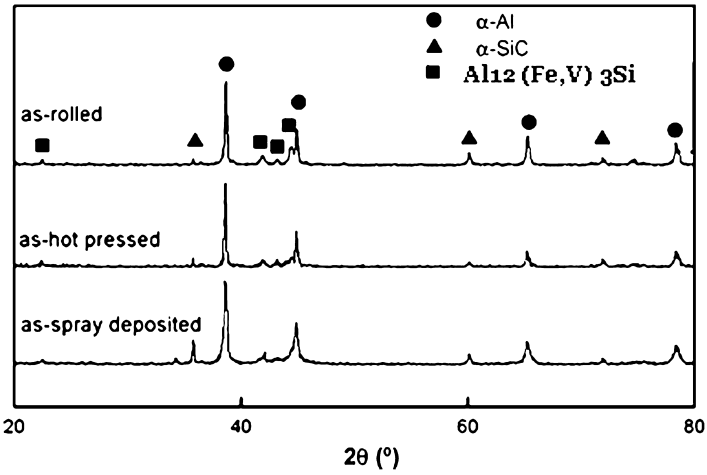

Figure 1. X-ray diffraction patterns of SiC_P/Al–Fe–V–Si composite as-deposited, as-hot pressed and as-rolled after hot pressed (hot pressed and rolled at 490°C).

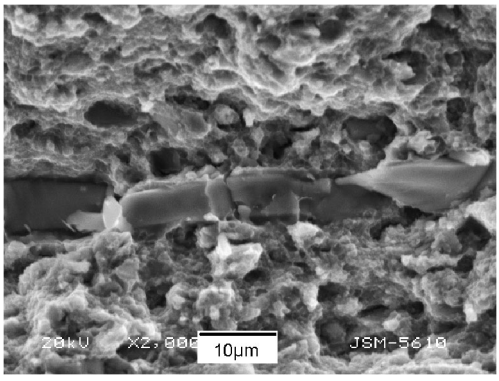

Figure 2. The fractograph of SiC_P/Al–11.7Fe–1.3V–1.7Si composite at 200°C.

phase and α-$Al_{12}(Fe, V)_3Si$ phase. No new peak appeared during the following hot work, and it suggested that the dispersion of the α-$Al_{12}(Fe, V)_3Si$ phase kept steady and free from transformation to γ-$Al_{13}Fe_4$ phase during hot work (up to 490°C). Figure 2 gives the fractograph of SiC_P/Al–11.7Fe–1.3V–1.7Si composite tested at 200°C, in which new smooth surface of SiC particle formed at the fracture can be seen. So it can be safely concluded that SiC particles have undergone tremendous load transferred from the Al matrix which leads to the fracture of SiC particles, which can enhance the composite.

Figure 3(a) exhibits the metallographic structure of SiC_P/Al–11.7Fe–1.3V–1.7Si composite, from which we can see that SiC particles distribute homogeneously in the Al matrix. Figure 3(b) presents the microstructures of the composite samples, which exhibits the shape and the size and the distribution of the Al grain and α-$Al_{12}(Fe, V)_3Si$. Both of them can be determined by means of SAD. From

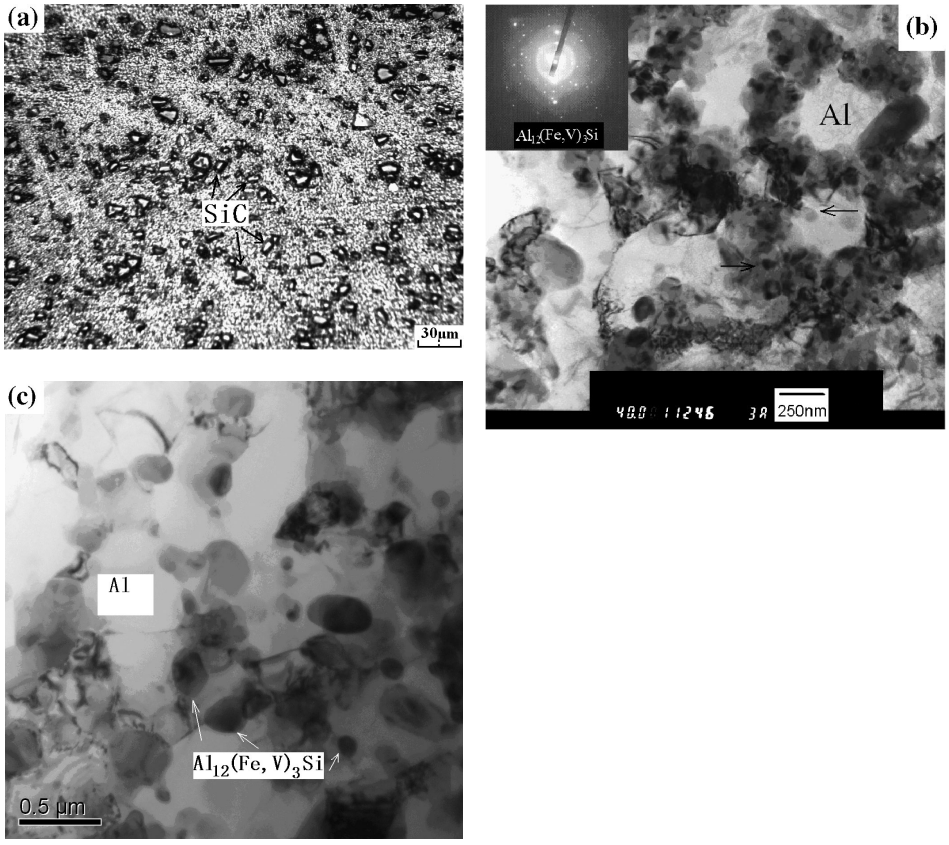

Figure 3. Metallographic and TEM micrographs of SiC_P/Al–11.7Fe–1.3V–1.7Si composite: (a)–(b) as-rolled; (c) heat exposure at 620°C for 10 h.

Fig. 3(b), it can be seen that the α-$Al_{12}(Fe, V)_3Si$ dispersoid particles of nearly spherical shape distribute in the Al matrix grains and along the grain boundaries; the sizes of the dispersoid particles and grains are 30–80 nm and 300–400 nm, respectively. Additionally, the volume fraction of α-$Al_{12}(Fe, V)_3Si$ is about 30–40%. It is interesting to note that the mass of the α-$Al_{12}(Fe, V)_3Si$ dispersoids are aggregated and are mainly located along the grain boundaries which separates the Al grains from each other. By investigation of the microstructure of Al–11.7Fe–1.15V–2.3Si, it can be found that it has a similar microstructure to that of spray deposited SiC_P/Al–11.7Fe–1.3V–1.7Si composite and the size of α-$Al_{12}(Fe, V)_3Si$ particles is about 50 nm [11]. Figure 3(c) presents the condition of SiC_P/Al–11.7Fe–1.3V–1.7Si composite as exposed to 620°C for 10 h. It is clear in Fig. 3(c) that the grain size has grown to 0.8–1 μm; most of the α-$Al_{12}(Fe, V)_3Si$ dispersoids grew up to 100–200 nm, while a small number grew up to 300–400 nm. The research for Al–12.4Fe–1.2V–2.3Si as-extruded alloy prepared by RS/PM suggested that most grains coarsened, a few grow up to 1 μm after heat exposure at 500°C for 100 h [12].

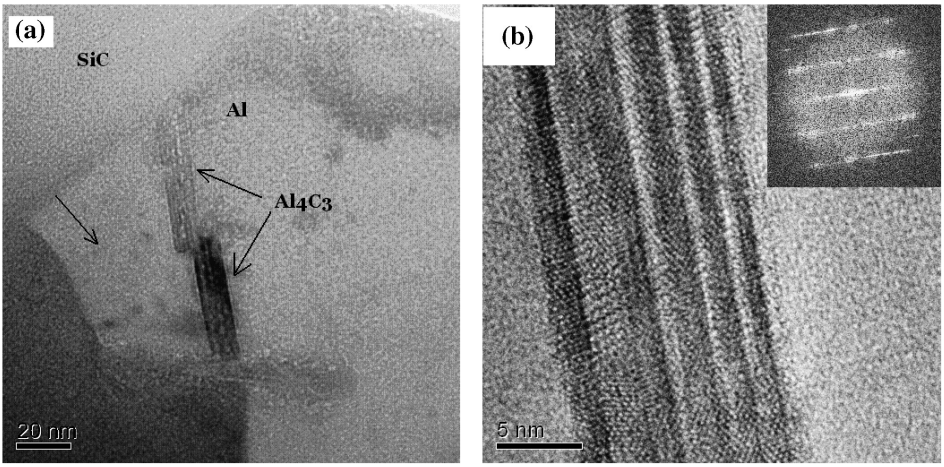

Figure 4. Al_4C_3 micrographs near the interface of Al matrix and SiC particle.

In our unpublished work, we found that the Si content was reducing gradually along the direction of the arrow in Fig. 4(a), which means that Si diffused from SiC particles into the Al matrix; in other words, the SiC particles reacted with the Al matrix. Based on all the information above, the following reaction on the interface of Al matrix and SiC particles during hot working and heat exposure can be formulated [13]:

$$\text{Al(in Al alloy)} + \text{SiC} \rightarrow \text{Al}_4\text{C}_3 + \text{Si(in Al alloy)} \quad (1)$$

As well known, reaction (1) exists in the Al/SiC composite universally [13–17] and the resultant products of reaction are definite. The formation of a cylindrical-shaped phase near the interface of Al matrix and SiC particles in SiC_P/Al–11.7Fe–1.3V–1.7Si composite after heat exposure at 620°C for 10 h can also be reported, as shown in Fig. 4(a) and 4(b). Analyzing FFT of the phase (on the right corner of Fig. 4(b)), the interplanar spaces were 0.34 nm and 0.28 nm, respectively, which were matched with that of (1 1 0) and (0 1 2) in Al_4C_3. Based on the analysis above, the cylindrical-shaped phase was determined as Al_4C_3. From Fig. 4(a), it can be seen that the Al_4C_3 phase is cylindrical-shaped, whose height and width are about 40 nm and 10 nm, respectively. Figure 4(b) is obtained by magnifying the Al_4C_3 phase in Fig. 4(a). From the height of the magnified image, it can be ascertained that the Al_4C_3 phase exhibited microtwin microstructure. Since the microtwin microstructure of Al_4C_3 phase has been characterized in paper [18], the characterization of Al_4C_3 phase is omitted here. Figure 5 presents the HREM images of the interface of Al matrix and reinforcement particle SiC. From the images, it is certain that the interface of the Al matrix and SiC particles is crystalline and the width of the interface is no more than 3 nm. The interface is rather planar and clean without any void. The orientation of the interface is different from that of Al matrix or SiC. By measuring the interplanar distance of the interface (Fig. 5(a)), it is clear that the interplanar distance is matching with (1 1 1) of Si. So it can be

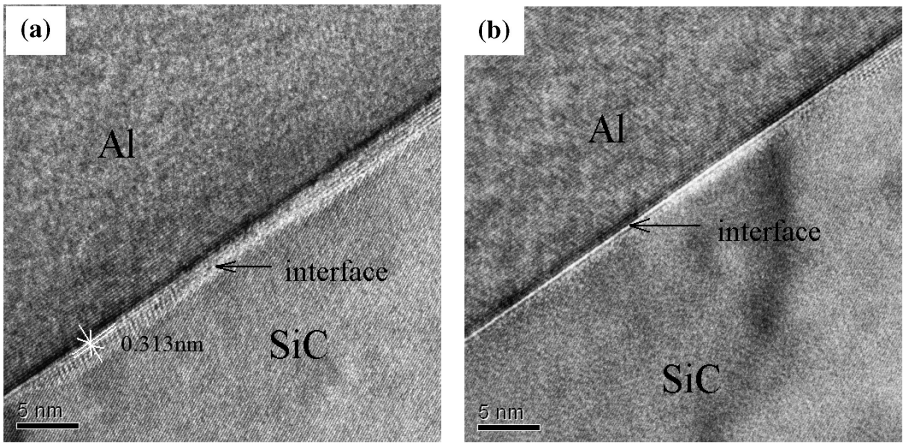

Figure 5. HREM micrographs of the interface of Al matrix and SiC particle.

Table 2.
The densities and relative densities of as-spray deposited, as-hot pressed and as-rolled SiC_P/Al–11.7Fe–1.3V–1.7Si composite

State	Experimental density (g/cm^3)	Theoretical density (g/cm^3)	Relative density (%)
As-spray deposited	2.682	3.031	88.4
As-hot pressed	2.988	3.031	98.6
As-rolled	3.029	3.031	99.9

safely concluded that the interface is made up of Si. Though the interface is narrow, the bonding is strong [19].

3.2. Relative Densities of SiC_P/Al–11.7Fe–1.3V–1.7Si Composites

Table 2 presents the relative densities of as-spray deposited, as-hot pressed, as-rolled SiC_P/Al–11.7Fe–1.3V–1.7Si composites. From the table, it can be seen that the relative density of SiC_P/Al–11.7Fe–1.3V–1.7Si remarkably increases after hot pressing and reach up to 98.6%, which illustrates that hot pressing is an effective process for densification. Furthermore, the state of full density was achieved throughout the rolling process.

3.3. Elevated Temperature Mechanical Properties of the Composite

Table 3 exhibits the mechanical properties of the samples of as-rolled SiC_P/Al–11.7Fe–1.3V–1.7Si composite measured at different temperatures. From the Table 3, it can be seen that the tensile strength (σ_b), yield strength ($\sigma_{0.2}$) and elongation (δ) of the composite samples are 315.8 MPa, 196.1 MPa and 2.5% at 315°C, respectively, while the figures are still up to 232.6 MPa, 127.7 MPa and 1.4% measured at 400°C.

Table 3.
The mechanical properties of SiC_P/Al–11.7Fe–1.3V–1.7Si composite at different temperatures

Tensile temperature (°C)	σ_b (MPa)	$\sigma_{0.2}$ (MPa)	δ (%)
25	581.2	518.4	4.5
100	461.5	362.7	4.2
150	396.5	286.9	3.5
200	372.2	221.2	3.3
250	347.8	282.3	2.8
315	315.8	196.6	2.5
350	255.8	219.1	2.7
400	232.6	127.7	1.4

Table 4.
Comparison of mechanical properties between SiC_P/Al–11.7Fe–1.3V–1.7Si (FVS1212) composite and Al–11.7Fe–1.3V–1.7Si alloy (SiC_P/FVS1212)

Alloys and composites	Ambient temperature properties (25°C)			Elevated temperature properties (315°C)		
	σ_b (MPa)	$\sigma_{0.2}$ (MPa)	δ (%)	σ_b (MPa)	$\sigma_{0.2}$ (MPa)	δ (%)
RS/PM FVS1212[20]	636	605	8.7	303	297	6.8
SD SiC_P/FVS1212	581	518	4.5	315	196	2.5

Table 4 lists the mechanical properties of spray-deposited SiC_P/Al–11.7Fe–1.3V–1.7Si composite and RS/PM Al–11.7Fe–1.3V–1.7Si alloy. The tensile strength of RS/PM Al–Fe–V–Si alloy is higher than that of SD alloys with the same chemical composition, due to the higher cool rate of rapid solidification than spray deposition. Compare with each other, it can be found that σ_b of spray-deposited SiC_P/Al–11.7Fe–1.3V–1.7Si composite is lower than that of RS/PM Al–11.7Fe–1.3V–1.7Si alloy under ambient temperature, but the former is higher than the latter at 315°C, which illustrates that SiC particles play a key role in enhancing the mechanical properties, especially elevated mechanical properties of the Al–11.7Fe–1.3V–1.7Si. The reinforcement mechanism will be discussed in the following discussion section.

3.4. Hardness Evolution

Figure 6 gives the evolution of the hardness of the SiC_P/Al–11.7Fe–1.3V–1.7Si composite as annealing time at different temperatures. From Fig. 6(a) to 6(c), it is found that the hardness of the composite samples had no evident drop at 350°C, 450°C and 550°C for 200 h. After exposure at 600°C for 10 h, the hardness of the composite fell slowly and the hardness still maintained onto 106 HB after 10 h

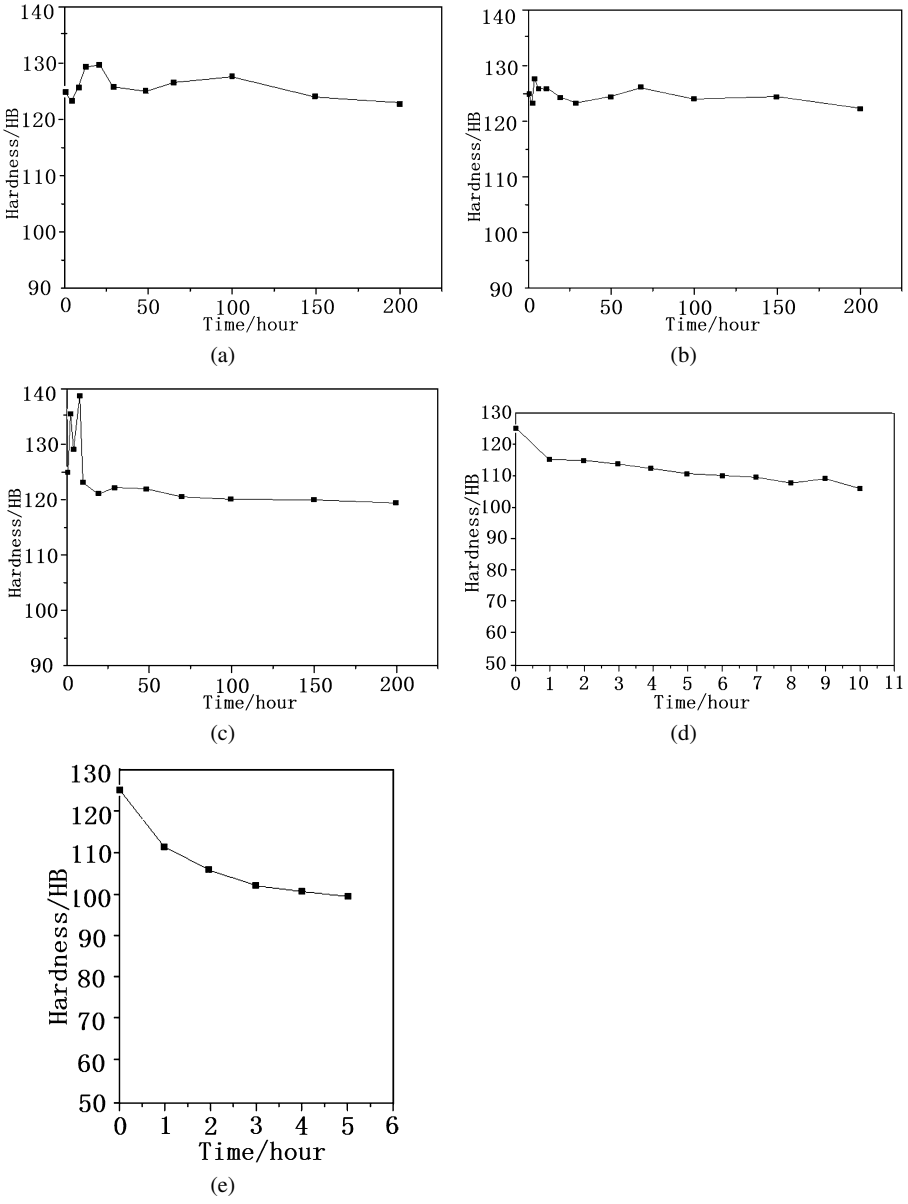

Figure 6. Room temperature hardness after annealing at certain temperatures for different time: (a) 350°C × 200 h, (b) 450°C × 200 h, (c) 550°C × 200 h, (d) 600°C × 10 h and (e) 620°C × 5 h.

(Fig. 6(d)). After annealing at 620°C for 5 h, the hardness of the composite sample fell more evidently than others and the hardness is below 100 HB (Fig. 6(e)). In our previous work [21], the hardness of the Al–8.5Fe–1.3V–1.7Si alloy samples prepared by the spray deposition technology showed no evident decline after exposure at 540°C for 100 h, 580°C for 2 h or 600°C for 1.5 h, but the hard-

ness dropped rapidly after exposure at 600°C more than 1.5 h. In addition, the hardness of SiC_P/Al–11.7Fe–1.3V–1.7Si composite prepared by spray deposition technology in our previous research declined rapidly after exposure at 620°C for 1 h. Paper [5] reported that the hardness of Al–8.4Fe–1.3V–1.7Si alloy prepared by multi-layer spray deposition dropped rapidly to 103 HB after exposure at 500°C for 200 h. Based on the above facts, it can be concluded that the thermal stability of SiC_P/Al–11.7Fe–1.3V–1.7Si composite prepared by spray deposition is excellent. The mechanics will be analyzed in the discussion.

3.5. Discussion

Rapidly solidified Al–Fe–V–Si alloys exhibit excellent elevated temperature mechanical properties, which should be attributed to the formation of the metastable α-Al_{12}(Fe, V)$_3$Si phase in the Al matrix. The α-Al_{12}(Fe, V)$_3$Si phase keeps steady up to 500°C and its coarsening rate is very low ($\nu = 8.4 \times 10^{-27}$ m^3/h under the condition of 425°C and the ratio of Fe and V is 10; while, $\nu = 2.9 \times 10^{-26}$ m^3/h when the ratio of Fe and V is 5) [22]. The α-Al_{12}(Fe, V)$_3$Si dispersoids are so concentrated on Al grain boundaries that they can hinder the growing and recrystallizing of Al grains when the environmental temperature rises. The plastic deformation of SiC_P/Al–11.7Fe–1.3V–1.7S composites happened by the sliding of the grain boundary under elevated temperature. The α-Al_{12}(Fe, V)$_3$Si particles can pin dislocations, and consequently delay the sliding of grain boundaries validly under high temperature.

Compared with rapidly solidified Al–Fe–V–Si alloys, spray-deposited SiC_P/Al–11.7Fe–1.3V–1.7S composite presents approximate elevated temperature mechanical properties, while the mechanical properties of Al–Fe–V–Si alloy prepared by rapid solidification and powder metallurgy are higher than that of the spray-deposited alloys generally. This is because the cooling rate of the rapid solidification process is higher than that of spray-deposition, which makes the sizes of the Al grains and α-Al_{12}(Fe, V)$_3$Si finer. The improvement of the spray-deposited SiC_P/Al–11.7Fe–1.3V–1.7S composite indicates that the introduction of SiC particles into the alloy is a key factor in increasing the mechanical properties. Now, special attention will be paid to the reinforcement mechanism of SiC particles. The following aspects are considered as the main strengthening mechanisms:

(1) The reaction between SiC particles and Al matrix plays a key role. Si released from SiC particles diffuses into the Al matrix, which changes the dissolved dynamic of α-Al_{12}(Fe, V)$_3$Si and reduces the coarsening rate of α-Al_{12}(Fe, V)$_3$Si, which makes it more difficult to form brittle $Al_{13}Fe_4$ [23]. Furthermore, the Si interface between SiC_P/Al increases the wettability between them, and thus improves the bonding of them. In addition, the dispersed Al_4C_3 phase is so fine that it can strengthen the composite through the proposed mechanism of dispersion strengthening [24, 25]. During heat exposure, the degree of the reaction increases as temperature rises, and more Si diffuses into the Al matrix, so the reaction plays a more important role in strengthening the composite.

(2) Load is transferred to SiC particles from Al matrix due to the mismatch in the elastic constants. From Fig. 2, it is certain that SiC particles are cut off during the tensile tests, which suggests higher load is needed when the breakage of SiC_P/Al–11.7Fe–1.3V–1.7S composite occurs.

(3) The bonding of SiC particles and Al matrix is strong. The fracture of as-rolled SiC_P/Al–11.7Fe–1.3V–1.7Si occurs at the position where the bonding is weak usually; however, there is strong bonding between SiC particles and Al matrix in the as-rolled composite, which can be seen from Figs 2 and 4. The crack extends when cutting through SiC particles and a new smooth surface of SiC particles forms (Fig. 2).

(4) The introduction of SiC particles increases the cooling rate of melt droplets when the particles insert into the drops during the atomization, which can refine the Al grain of the alloy matrix and the dispersion phase α-$Al_{12}(Fe, V)_3Si$ particles and increase their volume fraction. The finer Al grains and the higher volume fraction of dispersion particles of the composite compared to the alloy without reinforcement are important for strengthening the composite. The volume fraction was up to 30–40%. From Fig. 4, it can be seen that the size of the dispersoid particles and mean grain size are 30–80 and 300–400 nm, respectively. After exposure at 620°C for 10 h, the figures were 100–200 nm and 0.8–1 μm, respectively. Under such a high temperature, the coarsening rate of both was much lower compared with the alloy without SiC particle reinforcement. The strengthening resulted by the fining of grain size obeys the Hall–Petch equation:

$$\sigma_S = \sigma_0 + K_y d^{-1/2}, \tag{2}$$

where σ_0 and K_y are both constant, σ_0 is the resistance that the grain interior produces on formation, while d is the resistance grain boundary acts on formation. Because the value of d in SiC_P/Al–11.7Fe–1.3V–1.7Si composite increased more slowly than that of the alloy without SiC particle reinforcement, the elevated temperature mechanical properties and the thermal stability are improved. Under elevated temperature, the coarsening rate of α-$Al_{12}(Fe, V)_3Si$ and Al grains is relatively low, which resulted in the excellent mechanical properties and the good thermal stability.

(5) Solution strengthening: The average cooling rate was up to 2.55×10^4 K/s for a droplet of diameter in 100 μm flying to the disk in the course of spray deposition. Such a high cooling rate increases solid solubility of Fe atoms into the α-Al matrix, which was high to 4 at%, though it was only 0.025 at% in the condition of equilibrium freezing. The lattice parameter of α-Al increased because of the difference in atomic radius between Al and Fe, which resulted in the distortion of the lattice of α-Al phase and subsequently solution strengthening. Our previous work proved that the adding of SiC increased the cooling rate of

the melt droplets by accelerating the heat exchange of the melt droplets to the SiC particles, which can enhance solution strengthening further [26].

The above mechanics also impact on the elevated temperature mechanical properties of the composite simultaneously. At different temperature interval, point (1) affects the mechanical properties in different degrees. During elevated temperature, Si diffuses from SiC particles into the Al matrix more rapidly, which determines the influence that results from the reaction between Al matrix and SiC particles. This makes the influence on the mechanical properties more significant under these conditions; when the temperature is relatively low, the action is weaker. The other mechanics play a similar role at different temperature intervals.

4. Conclusions

(1) SiC_p/Al–11.7Fe–1.3V–1.7Si sheets prepared by spray deposition (SD)-hot pressing-rolling process exhibited excellent elevated temperature mechanical properties. For instant, σ_b was 315.8 MPa when tested at 315°C, but the figure was 232.6 MPa at 400°C. The addition of SiC particles into the Al–Fe–V–Si alloy made the composite exhibit similar elevated temperature mechanical properties compared to the rapidly solidified/powder metallurgy Al–Fe–V–Si alloy of similar composition without SiC particle reinforcement.

(2) SiC_p/Al–11.7Fe–1.3V–1.7Si sheets also presented high thermal stability. The hardness after heat exposure at 550°C for 200 h or 600°C for 10 h declined obscurely. The improvement of the thermal stability arises from the influence of SiC particles.

(3) In SiC_p/Al–11.7Fe–1.3V–1.7Si composite, a reaction between SiC particles and Al matrix occurred; an interface formed between Si and Al/SiC_P. Furthermore, some Si diffuses from SiC particles into the Al matrix with the formation of Al_4C_3. The diffusion of Si into the matrix stabilized the α-$Al_{12}(Fe, V)_3Si$ phase. Dispersed entwined Al_4C_3 particles are so fine that they can strengthen the matrix.

Acknowledgements

The research described in this publication was made possible by financial support of the Hunan Provincial Education Department (No. 08D127).

The authors would like to acknowledge the contribution of Mr. G. Chen, Mr. J. Z. Liu of Hunan University to the research. Thanks are given to Dr. D. Chen, Dr. Y. P. Sun, Dr. H. Zhang and Dr. W. J. Xia.

References

1. D. J. Skinner, R. L. Bye, D. Raybould and A. M. Brown, Dispersion strengthened Al–Fe–V–Si alloys, *Scripta Metallurgica* **20**, 867–872 (1986).

2. S. Hariprasad, S. M. L. Sastry, K. L. Jerina and R. J. Lederich, Microstructures and mechanical properties of dispersion-strengthened high-temperature Al–8.5Fe–1.2V–1.7Si alloys produced by atomized melt deposition process, *Metall. Trans. A* **24**, 865–873 (1993).
3. S. C. Khatri, A. Lawley, M. J. Koczak and K. G. Grassett, Creep and microstructural stability of dispersion strengthened Al–Fe–V–Si–Er alloy, *Mater. Sci. Engng A* **167**, 11–21 (1993).
4. U. Prakash, T. Raghu, A. A. Gokhale and S. V. Kamat, Microstructure and mechanical properties of RSP/M Al–Fe–V–Si and Al–Fe–Ce alloys, *J. Mater. Sci.* **34**, 5061–5065 (1999).
5. M. N. Srinivasan and S. D. Little, Effect of melt spinning variables on the structure and properties of a dispersion strengthened Al–Fe–V–Si alloy, *Scripta Metall. Mater.* **32**, 1153–1158 (1995).
6. K. L. Sahoo, S. K. Das and B. S. Murty, Formation of novel microstructures in conventionally cast Al–Fe–V–Si alloys, *Mater. Sci. Engng A* **355**, 193–200 (2003).
7. J. Čadek, K. Kuchařová and S. J. Zhu, High temperature creep behavior of an Al–8.5Fe–1.3V–1.7Si alloy reinforced with silicon carbide particulates, *Mater. Sci. Engng A* **283**, 172–180 (2000).
8. S. Yaneva, A. Kalkanlı, K. Petrov, R. Petrov, Ir. Yvan Houbaert and S. Kassabov, Structure development in rapidly solidified Al–Fe–V–Si ribbons, *Mater. Sci. Engng A* **373**, 90–98 (2004).
9. F. Carreño, M. T. Pérez-Prado, G. González-Doncel and O. A. Ruano, Texture stability of a rapidly solidified dispersion strengthened Al–Fe–V–Si material, *Scripta Mater.* **38**, 1427–1433 (1998).
10. B. Lu, D. Q. Yi, W. X. Li, Z. M. Yu and L. Zhu, Thermal stability of multi-spray deposition heat resistant Al–Fe–V–Si alloy, *Trans. Nonferr. Metals Soc. China* **12**, 273–276 (2002).
11. I. S. Kim, N. J. Kim and S. W. Nam, Temperature dependence of the optimum particle size for the dislocation detachment controlled creep of Al–Fe–V–Si/SiC_P composite. *Scripta Metall. Mater.* **32**, 1813–1819 (1995).
12. R. E. Franck and J. A. Hawk, Effect of very high temperatures on the mechanical properties of Al–Fe–V–Si alloy, *Scripta Metall.* **23**, 113–118 (1989).
13. J. C. Lee, H. K. Seok and H. I. Lee, Alloy design of thixoformable wrought SiC/Al alloy composites, *Mater. Res. Bull.* **34**, 35–41 (1999).
14. M. Sherif El-Eskandarany, Mechanical solid state mixing for synthesizing of SiC/Al nanocomposites, *J. Alloys Compounds* **279**, 263–271 (1998).
15. J. C. Lee, J. Y. Byun, H. K. Seok, C. S. Oh and H. I. Lee, Prediction of Si contents to suppress the formation of Al_4C_3 in the SiCP/Al composite, *Acta Mater.* **46**, 1771–1780 (1998).
16. D. S. Shin, J. C. Lee, E. P. Yoon and H. I. Lee, Effect of the processing methods on the formation of Al_4C_3 in SiC_P/2024Al composites, *Mater. Res. Bull.* **32**, 1155–1163 (1997).
17. J. K. Park and J. P. Lucas, Moisture effect on SiC_P/6061Al MMC: dissolution of interfacial Al_4C_3, *Scripta Mater.* **37**, 511–516 (1997).
18. J. B. Wen, J. M. Zhang, W. Zhang, Z. Q. Zhang, Y. H. Zhang and H. F. Zhang, The crystallographic features of Al_4C_3 phase in hot-dip aluminized steel, *Trans. Mater. Heat Treatment* **27**, 75–78 (2006).
19. J. C. Romero and R. J. Arsenault, Anomalous penetration of Al into SiC, *Acta Metall. Mater.* **43**, 849–857 (1995).
20. M. J. Couper, J. W. Luster and M. Thumann, Development of elevated temperature powder metallurgy aluminum alloys, *Powder Metall. Intl* **23**, 7–151 (1991).
21. M. Y. Zhan, Z. H. Chen and W. J. Zia, Effects of high temperatures on the hardness and microstructure of spray-deposited heat-resistant 8009 aluminum alloy, *J. Mater. Engng* **3**, 35–37 (2004).
22. P. S. Gilman and S. K. Das, Rapidly solidified aluminum alloys for high temperature/high stiffness applications, *Metal Powder Report* **44**, 616–620 (1989).

23. R. Hambleton, H. Jones and W. M. Rainforth, Effect of alloy composition and reinforcement with silicon carbide on the microstructure and mechanical properties of three silicide dispersion strengthened aluminium alloys, *Mater. Sci. Engng A* **304–306**, 524–528 (2001).
24. V. Garibay-Febles, H. A. Calderon, F. C. Robles-Hernández, M. Umemoto, K. Masuyama and J. G. Cabañas, Production and characterization of (Al, Fe)–C (graphite or fullerene) composites prepared by mechanical alloying, *Mater. Manuf. Proc.* **15**, 547–576 (2000).
25. M. Besterci, Preparation, microstructure and properties of Al–Al_4C_3 system produced by mechanical alloying, *Materials and Design* **27**, 416–421 (2006).
26. Z. H. Chen, Y. Q. He, H. G. Yan, Z. G. Chen, X. J. Yin and G. Chen, Ambient temperature mechanical properties of Al–8.5Fe–1.3V–1.7Si/SiC_P composite, *Mater. Sci. Engng A* **460–461**, 180–185 (2007).